**Atmospheric
Chemistry
and Physics**

Quantifying the magnitude of a missing hydroxyl radical source in a tropical rainforest

L. K. Whalley[1,2]**, P. M. Edwards**[1]**, K. L. Furneaux**[1, †]**, A. Goddard**[1]**, T. Ingham**[1,2]**, M. J. Evans**[3]**, D. Stone**[1]**,
J. R. Hopkins**[4,5]**, C. E. Jones**[4,5]**, A. Karunaharan**[6]**, J. D. Lee**[4,5]**, A. C. Lewis**[4,5]**, P. S. Monks**[6]**, S. J. Moller**[4]**, and
D. E. Heard**[1,2]

[1]School of Chemistry, University of Leeds, Woodhouse Lane, Leeds, LS2 9JT, UK
[2]National Centre for Atmospheric Science, University of Leeds, Leeds, LS2 9JT, UK
[3]School of Earth and Environment, University of Leeds, Woodhouse Lane, Leeds, LS2 9JT, UK
[4]Chemistry Department, University of York, Heslington, YO10 5DD, UK
[5]National Centre for Atmospheric Science, University of York, Heslington, YO10 5DD, UK
[6]Department of Chemistry, University of Leicester, University Road, Leicester, LE1 7RH, UK
[†]Sadly passed away on 28 July 2009

Abstract. The lifetime of methane is controlled to a very large extent by the abundance of the OH radical. The tropics are a key region for methane removal, with oxidation in the lower tropical troposphere dominating the global methane removal budget (Bloss et al., 2005). In tropical forested environments where biogenic VOC emissions are high and NO_x concentrations are low, OH concentrations are assumed to be low due to rapid reactions with sink species such as isoprene. New, simultaneous measurements of OH concentrations and OH reactivity, k'_{OH}, in a Borneo rainforest are reported and show much higher OH than predicted, with mean peak concentrations of $\sim 2.5 \times 10^6$ molecule cm^{-3} (10 min average) observed around solar noon. Whilst $j(O^1D)$ and humidity were high, low O_3 concentrations limited the OH production from O_3 photolysis. Measured OH reactivity was very high, peaking at a diurnal average of 29.1 ± 8.5 s^{-1}, corresponding to an OH lifetime of only 34 ms. To maintain the observed OH concentration given the measured OH reactivity requires a rate of OH production approximately 10 times greater than calculated using all measured OH sources. A test of our current understanding of the chemistry within a tropical rainforest was made using a detailed zero-dimensional model to compare with measurements. The model over-predicted the observed HO_2 concentrations and significantly under-predicted OH concentrations. Inclusion of an additional OH source formed as a recycled product of OH initiated isoprene oxidation improved the modelled OH agreement but only served to worsen the HO_2 model/measurement agreement. To replicate levels of both OH and HO_2, a process that recycles HO_2 to OH is required; equivalent to the OH recycling effect of 0.74 ppbv of NO. This recycling step increases OH concentrations by 88 % at noon and has wide implications, leading to much higher predicted OH over tropical forests, with a concomitant reduction in the CH_4 lifetime and increase in the rate of VOC degradation.

1 Background

OH radicals are responsible for the removal of the majority of reactive trace gases emitted into the atmosphere (Heard and Pilling, 2003; Monks, 2005). In remote, background environments, far from anthropogenic emissions, OH is primarily produced by the photolysis of O_3 and the subsequent reaction of $O(^1D)$ atoms with H_2O vapour:

$$O_3 \xrightarrow{h\nu (<340 \text{ nm})} O(^1D) + O_2 \tag{R1}$$

$$O(^1D) + H_2O \rightarrow 2OH \tag{R2}$$

The photolysis of other trace gases, for example HONO and H_2O_2 can also act as direct OH sources. Reactions of O_3 with alkenes may contribute to OH formation in the daytime and these reactions may be a significant source of the radical at night in the absence of photolytic sources (Salisbury et al., 2001). In the presence of NO, HO_2 can also be recycled back

to OH. In contrast to these relatively few well defined OH sources, in all but the cleanest of background environments there are a multitude of OH sinks, and, due to the large variety of these, it becomes virtually impossible to measure each explicitly. In tropical rainforests, the emissions of highly reactive biogenic VOCs are large. Global modelling studies estimate that such biogenic emissions may significantly reduce the oxidising capacity in tropical forests (Lelieveld et al., 2002; Lelieveld et al., 2004), and, in turn, extend the lifetime of CH_4 in these areas considerably. In contrast to model predictions, field studies in mid-latitude forests (Carslaw et al., 2001; Tan et al., 2001), and more recently in tropical rainforests (Lelieveld et al., 2008; Butler et al., 2008; Kubistin et al., 2010; Martinez et al., 2010) and other tropical locations (Hofzumahaus et al., 2009) have found that appreciable concentrations of OH are maintained even in the presence of high biogenic emissions indicating that OH sources are not properly captured by models under certain chemical conditions.

Thornton et al. (2002) first suggested that uncertainties in the product of the branching ratio and/or rate constant for organic peroxide formation from $HO_2 + RO_2$ reactions could be a cause for large modelled/measured OH discrepancies. Lelieveld et al. (2008) extended this idea, proposing that the source of unpredicted OH over Amazonia may derive from the reaction of HO_2 with organic peroxy radicals (formed via isoprene oxidation) directly forming OH. In support of this, several studies have highlighted that the modelled/measured discrepancy increases as a function of isoprene (Ren et al., 2008; Kubistin et al., 2010). Modelling studies suggest that between 2 to 3.2 OH radicals need to be recycled from these reactions to reproduce the OH mixing ratios measured over Amazonia (Butler et al., 2008; Kubistin et al., 2010). However, kinetic studies of reactions of HO_2 with a number of peroxy radicals do not support such high OH yields (Hasson et al., 2004; Dillon and Crowley, 2008).

A number of novel mechanisms that provide a significant yield of OH following the OH initiated oxidation of isoprene have recently been reported, determined by theoretical *ab initio* calculations (Peeters et al., 2009; Da Silva et al., 2010; Nguyen et al., 2010) or by laboratory studies (Paulot et al., 2009). The mechanism of Peeters et al. (2009) postulates an OH radical yield of ∼1 per isoprene molecule oxidised; more recent publications (Stravrakou et al., 2010; Peeters & Muller, 2010) assume that an OH yield of up to 3 may be possible and, as such, has the greatest potential to sustain the oxidising capacity in rainforests. Calculations suggest that if an OH yield of 3 from isoprene oxidation were to be included in the MECCA modelling scheme used in the GABRIEL project, the OH model under-prediction could be rectified (Peeters et al., 2009; Archibald et al., 2010; Stavrakou et al., 2010). During the PRIDE-PRD campaign, Hofzumahaus et al. (2009) excluded additional HO_x initiation pathways, as their inclusion in model calculations caused an overestimation in the previously well replicated HO_2 concentra-

tions. Instead, Hofzumahaus et al. (2009) proposed that the additional OH source could derive from the recycling of RO_2 radicals to HO_2 and subsequently of HO_2 radicals to OH via reaction with unidentified species. A similar observation was also made by Tan et al. (2001) during the PROPHET 98 campaign, in which the measured OH concentrations were, on average, a factor of 2.7 times greater than modelled concentrations, whilst the HO_2 modelled and measured concentrations were in reasonable agreement, suggesting a missing process converting HO_2 to OH rather than a missing direct OH source.

Pugh et al. (2010) have used the Cambridge tropospheric trajectory model of chemistry and transport (CiTTyCAT) (Wild et al., 1996) to assess the chemistry of the Borneo rainforest during the Oxidants and Particle Photochemical Processes (OP3) project and suggest a reduction of 50 % in the effective rate coefficient for reaction of OH with isoprene (caused by incomplete mixing of isoprene-rich air-parcels) is able to resolve the underestimation of OH whilst maintaining agreement between measured isoprene, MVK and MACR concentrations and isoprene fluxes. However, more recently the degree of isoprene OH separation was determined to be no greater than 15 % (Pugh et al., 2011).

In this paper, we make use of measurements of OH, HO_2, OH reactivity and ancillary species and radiation parameters that are involved in the production of OH, to investigate the closure of the HO_x budget and make a first quantitative assessment of the magnitude of unrepresented sources. All data reported in this paper were recorded during the OP3 project that took place in the Malaysian Borneo rainforest (Hewitt et al., 2010).

2 Experimental

Measurements were performed during the OP3 field campaign (Hewitt et al., 2010) in 2008 at Bukit Atur Global Atmospheric Watch station (5.0° N, 117.8° E), in Danum Valley, located in the Sabah region of the Borneo rainforest. The campaign consisted of two intensive four week measurement periods run during April (OP3-I) and July (OP3-III); OH reactivity measurements were made during the April intensive only. Co-located measurements of VOCs (measured using Gas Chromatography-Flame Ionisation Detection, Hopkins et al., 2003), O_3 (UV absorption, Martin et al., 2006), NO, NO_2 (chemiluminescence and photolytic converter, Martin et al., 2006), $j(O^1D)$ (filter radiometry, Bohn et al., 2008), OH (Fluorescence Assay by Gas Expansion – details below) and OH reactivity (details below) were made in a forest clearing from the roof of a 6 m (length) shipping container located on a flat-bed trailer, at a height of approximately 5 m. The surrounding tree tops were at a height of ∼10 m and the container was located ∼10 m from the forest edge. The measurement inlets for OH and OH reactivity were in full sunlight from approximately 06:00–18:00 local time (LT). The sum

of HO$_2$+RO$_2$ were detected at a height of ∼5 m using the PEroxy Radical Chemical Amplification (PERCA) technique (Fleming et al., 2006), from the roof of a second shipping container displaced ∼20 m from the OH measurement container. The measurement of the sum of HO$_2$+RO$_2$ has been used to assess the potential importance of an OH source from reaction of RO$_2$ radicals with HO$_2$ radicals. A rate coefficient, $k_{HO_2+RO_2} = 2.05 \times 10^{-13} e^{(1300/T)}$ cm^3 molecule^{-1} s^{-1} which is the Master Chemical Mechanism (MCM) recommendation for reaction of isoprene derived peroxy radicals with HO$_2$, is used in these calculations.

A number of measurements used in the Photostationary Steady State (PSS) analyses (Sect. 3) were limited or missing during the April intensive, in some cases data taken during the second measurement period have been utilised to provide an estimate of typical values of these species in this environment. For example, such an approach has been employed for HO$_2$ concentration measurements, which were not made during the first measurement period owing to the unavailability of nitric oxide gas to convert HO$_2$ to OH for subsequent detection. The average diurnal profile of HO$_2$ measured during OP3-III was used in the PSS. $j(O^1D)$ was measured from the roof of the OH measurement container using a filter radiometer (Bohn et al., 2008) throughout both intensives. Similar peak photolysis rates were observed during both measurement periods although increased cloud cover during the second campaign led to more frequent brief reductions in $j(O^1D)$. The photolysis rates of other species such as j(peroxides) have been calculated using the Tropospheric Ultraviolet and Visible (TUV) radiation model (Madronich and Flocke, 1998). The correlation between TUV calculated j(peroxides) with TUV calculated $j(O^1D)$ was determined allowing these photolysis rates to be scaled to the measured $j(O^1D)$ values to account for passing clouds. The presence of clouds is likely to affect the photolysis rates of these chemical species by different amounts adding an additional uncertainty into the calculations performed. No peroxide measurements were made during either intensive period. A constant concentration in the PSS analyses has been assumed for H$_2$O$_2$ and organic peroxides (we have assumed that the total organic peroxides are all CH$_3$OOH) of 2.41 ppbv and 0.96 ppbv, respectively, which represent measured concentrations of these species that were made in the boundary layer over Amazonia during the GABRIEL campaign (Lelieveld et al., 2008). The OH yield of 0.26 from O$_3$-isoprene reactions was taken from recent recommendations (Malkin et al., 2010).

HONO was not measured during OP3-I; low concentrations of HONO (peak concentration was ∼15 pptv, Pugh et al., 2011) were detected during OP3-III, however. At these mixing ratios, the photolysis of HONO has a negligible impact as an OH source and, as such, is not included in the results presented on this paper.

2.1 OH and HO$_2$ measurements

OH was measured using the fluorescence assay by gas expansion (FAGE) technique, and details of the experimental arrangement can be found in Whalley et al. (2010). Air was drawn into a large cylindrical, stainless steel cell via a 1 mm diameter nozzle sat upon a 5 cm tall turret. The cell was maintained at 0.9 Torr. The OH radicals were electronically excited at ∼308 nm using a tuneable, pulsed laser. The fluorescence at the same wavelength was detected perpendicular to the laser axis using a channel photo-multiplier (CPM) and gated photon counting. The sensitivity of the cell towards OH was calibrated using VUV photolysis of H$_2$O vapour in a flow of zero air, coupled to O$_2$ actinometry, to generate a known quantity of OH radicals. Data were collected every 10 s and then averaged up to the 10 min radical concentrations presented here. The average limit of detection (LOD) of the system during the campaign was ∼1.95 $\times 10^5$ molecule cm^{-3} (10 min data collection period), with an associated uncertainty due to the accuracy of the calibration of ∼15 % (1σ). HO$_2$ may also be detected using the FAGE technique by first titrating HO$_2$ to OH by the addition of small quantities (∼30 sccm) of NO (99.5 %, BOC) above the excitation region and this method was employed to detect HO$_2$ during the second intensive. The HO$_2$ measurements made in OP3-III and used in the subsequent analysis are taken during periods when local NO$_x$ concentrations were not elevated from natural background levels.

2.2 OH reactivity

OH reactivity (k'_{OH}) was measured using an apparatus which has been described in detail by Ingham et al. (2009). Ambient air was drawn into a 2 m long, 10 cm internal diameter PVC flow tube at a rate of 300 L/min, generating a turbulent flow. OH was generated by 185 nm photolysis of H$_2$O vapour in a N$_2$ flow and introduced into the flow tube via a sliding injector, and was detected downstream in the flowtube using a second FAGE cell. Increasing the distance (and, therefore, time, t as the flow-velocity was known) between the point of injection and the FAGE sampling point enables the decay of OH to be recorded, which was found to be exponential and is described by:

$$[OH]_t = [OH]_0 e^{(-(k'_{OH}+k'_{physical})t)} \tag{1}$$

where $k'_{physical} = 6.1 \pm 0.65$ s^{-1} is the physical OH loss rate. $k'_{physical}$ was determined post-campaign by replacing the ambient air flow with an extremely clean flow of gas and recording the subsequent decay (P. M. Edwards, personal communication, 2011).

2.3 Box model incorporating the Master Chemical Mechanism

The Dynamically Simple Model of Atmospheric Chemical Complexity (DSMACC) zero-dimensional box model (Stone et al., 2010) has been used to estimate HO_2 concentrations for comparison with the ambient HO_2 concentrations measured during OP3-III. The chemistry scheme, generated by the Master Chemical Mechanism (Carslaw et al., 2001), includes near explicit degradation schemes for the observed hydrocarbons, isoprene, α-pinene, C_2H_6, C_2H_4, C_3H_8, C_3H_6, iC_4H_{10}, $n-C_4H_{10}i-C_5H_{12}$, $n-C_5H_{12}$, $n-C_6H_{14}$ and C_2H_2. Rate coefficients for inorganic reactions and three body reactions were updated to recent recommendations. Simulations were integrated forwards using a Rosenbrock solver (Hairer and Wanner, 1991) with a timestep of 600 s until a diurnal steady state was reached, at which point the diurnal cycles of simulated species were considered to exhibit less than 0.01 % variation from day to day.

Simulations were constrained to the observed average diurnal cycles of O_3, NO, NO_x, CO, H_2O vapour, $j(O^1D)$, temperature and the observed hydrocarbons listed above for all days of OP3-I, averaged into 30 min time bins. The modelled HO_2 was compared to one day of HO_2 measurements taken during OP3-III. This day was chosen for comparison with the model as the concentrations of auxiliary measurements on this day were similar to the measurement values used as model constraints. The mean total peroxy radicals (HO_2+RO_2) concentrations, as detected using the PERCA method (Fleming et al., 2006), were similar during OP3-I and OP3-III supporting the assumption that the OP3-I HO_2 concentrations were likely similar to the HO_2 concentrations recorded during OP3-III. NO_2 and total NO_x were the only constrained species permitted to vary during each 24 h period in the model with their concentrations constrained in such a way as to constrain the NO_2 to its observed value at the end of each 24 h period in the model whilst maintaining the modelled partitioning between NO_x species. NO was constrained to its observed concentration at the beginning of the model run and then permitted to vary with the constraints placed on NO_2 and total NO_x. This approach has been employed previously by Ren et al. (2008) and Stone et al. (2010). The methane concentration in the model was set to 1770 ppbv and the hydrogen concentration was set to 550 ppbv (Novelli et al., 1999; Ehhalt and Rohrer, 2009).

Photolysis rates, except for $j(O^1D)$, which was measured, were calculated using the tropospheric ultraviolet and visible (TUV) radiation model at solar zenith angles (SZA) between 0 and 90° in 5° steps. Spline fits were applied to the calculated photolysis rates as a function of SZA, and the appropriate photolysis rates selected for the SZA. Calculated photolysis rates were subsequently scaled to the mean ratio of TUV calculated and observed $j(O^1D)$. A surface albedo of 0.1 (Govaerts et al., 2008) was used for all model runs.

In order to prevent the build-up of long-lived unconstrained species such as H_2O_2 and other peroxides in the model, a deposition lifetime was applied to all calculated species, to represent physical loss of species either through deposition or mixing. As there are no observations of these species to allow a true deposition rate to be estimated, a rate coefficient for the deposition process of $1 \times 10^{-5}\,\mathrm{s^{-1}}$ was chosen for all runs presented here, corresponding to a deposition lifetime of 24 h; the modelled HO_2 concentration increases by 14 % if the deposition lifetime increases to 48 h. The sensitivity of the model to this parameter is further discussed by Stone et al. (2010).

3 Results and discussion

The average diurnal profile, constructed from 25 days of OH measurements during the first OP3 campaign (OP3-I), and shown in Fig. 1, is used in all subsequent analyses. The 1σ standard deviation of this averaged profile is mainly due to the variability of the data from day-to-day caused by variability in chemical composition, but also contains a contribution from instrumental precision. The corresponding average diurnal profiles of NO, O_3, $j(O^1D)$, isoprene and OH reactivity, k'_{OH}, all of which influence the OH profile, are also shown in Fig. 1 for the OP3-I campaign. The mean daytime isoprene concentration of $\sim$1.9 ppbv (averaged between 06:00–18:00 LT) measured during OP3-I is comparable to isoprene measurements made in the boundary layer over the Suriname rainforest during the GABRIEL project (mean daytime isoprene $\sim$2 ppbv observed, Lelieveld et al., 2008). Only 2 h of OH reactivity data were taken during the GABRIEL project due to an instrument failure making it difficult to compare the mean diurnal levels. Peak OH reactivities, however, were similar ($72\pm18\,\mathrm{s^{-1}}$ and $83.6\pm26.0\,\mathrm{s^{-1}}$ (single points)) during GABRIEL (Sinha et al., 2008) and OP3 respectively. NO concentrations are also similar ($\sim$0.02 ppbv) to those measured during the GABRIEL project (Lelieveld et al., 2008) at all times other than at sunrise when a reproducible spike in NO peaking at $\sim$0.2 ppbv was observed during the OP3 project (Fig. 1); please refer to Pike et al. (2010) for further details on the OP3-I NO profile. Both O_3 concentration and O_3 photolysis rates were higher over the Suriname forest ($O_3\sim$18.5 ppbv, mean daytime concentration and $j(O^1D)$ $\sim$6.3$\times10^{-5}\,\mathrm{s^{-1}}$ at solar noon, Martinez et al., 2010) than in the Borneo forest (Fig. 1) indicating that the rate of primary production of OH from the photolysis of O_3 and subsequent reaction with H_2O vapour was higher during the GABRIEL project than OP3. The factor of two difference in noontime $j(O^1D)$ between OP3 and GABRIEL is surprising given the similar latitudes of the two field projects. The lower $j(O^1D)$ observed during OP3 may be partially explained by cloud-cover and measurement height, i.e. ground observations (OP3) vs aircraft measurements (GABRIEL). It is likely also that the proximity of the surrounding trees
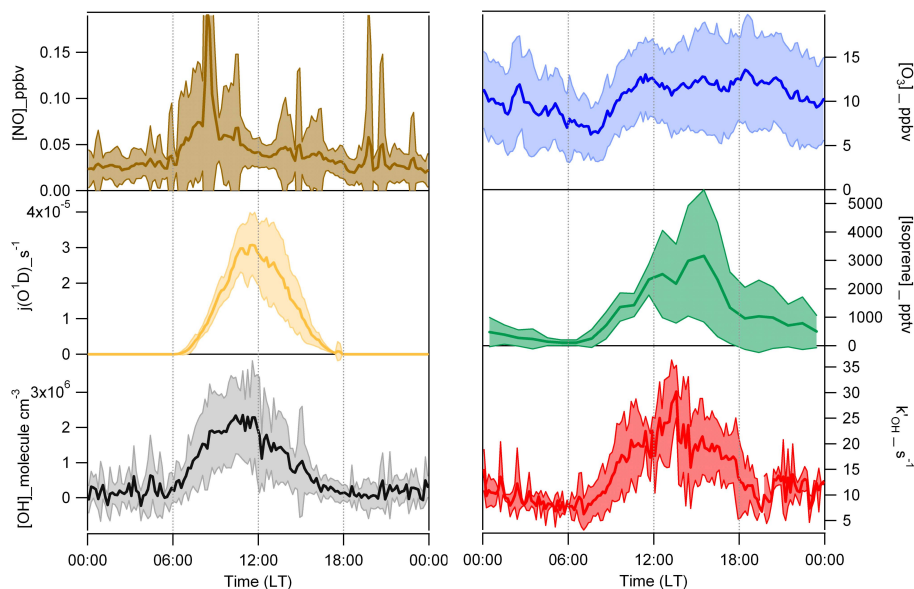
Fig. 1. Average diurnal profile of key species during OP3-I generated from 10 min data taken over 25 days (from the 6 April 2008–2 May 2008) for OH, k'_{OH}, $j(O^1D)$, NO and O_3, and over 25 days from hourly data for isoprene. The shaded areas show the 1σ day-to-day variability of the data used to generate the mean diurnal profiles.

Table 1. Description of the scenarios used in the text and figures and the impact of the different OH source terms in the PSS approximation Eq. (4). The colours of the lines in the symbol column correspond to the $[OH]_{calc}$ diurnal profile shown in Fig. 2 calculated using the different Scenarios (1–5). $[OH]_{calc}$:$[OH]_{meas}$ ratio represents the mean ratio over 24 h for all scenarios apart from Scenario 4. f is the fraction of $O(^1D)$ that reacts with H_2O vapour to form OH, rather than being quenched to $O(^3P)$.

Scenario	$\Sigma OH_{sources}$	Symbol (Fig. 2)	$\frac{[OH]_{calc}}{[OH]_{meas}}$
(1)	$2j(O^1D)[O_3][H_2O]f$	—	0.05
(2)	$(1)+k_{NO+HO_2}[HO_2][NO]+k_{O_3+HO_2}[O_3][HO_2]+0.26k_{O_3+C_5H_8}[O_3][C_5H_8]+$ $2j(H_2O_2)[H_2O_2]+j(CH_3OOH)[ROOH]$	—	0.15
(3)	$(2)+k_{C_5H_8+OH}[C_5H_8][OH]$	—	0.37
(4)	$(2)+2.7\times k_{C_5H_8+OH}[C_5H_8][OH]$	—	1.0*
(5)	$(2)+k_{X+HO_2}[X][HO_2]$ ($[X]=0.74$ ppbv)	—	1.0

* $[OH]_{calc}$:$[OH]_{meas}$ = 1 during afternoon and evening hours only (noon–midnight).

may have reduced the actinic flux at the Bukit Atur site somewhat. Comparison of the $j(O^1D)$ measurements made using the filter radiometer and a spectral radiometer (deployed during OP3iii) were is excellent agreement, providing confidence that the photolysis rates used in the subsequent calculations are accurate. The higher primary rate of production experienced during GABRIEL likely results in the higher daytime mean OH concentrations observed during the project ($\sim5.6\times10^6$ molecule cm^{-3}) than during OP3 ($\sim1.2\times10^6$ molecule cm^{-3}) (Fig. 1). One of the most notable results from the OP3 project is that significant OH concentrations are maintained despite a high OH reactivity, defined by $k'_{OH}=\Sigma k'_{OH+Y}[Y]$, where Y represents an OH sink, suggesting that there are significant OH sources present.

The short lifetime of OH (daytime mean of ~59 ms, Fig. 1) indicates that OH exists in a photostationary steady state, where OH production is balanced by OH loss. Simultaneous measurements of OH concentration and k'_{OH} enable "measurement" of the total rate of OH production, $\Sigma OH_{sources}$ using:

$$\Sigma OH_{sources} = [OH] \times k'_{OH} \qquad (2)$$

In many environments the major source of OH is from the reaction of $O(^1D)$ with water vapour, the rate of which is given by:

$$p(OH) = 2 \times j(O^1D) \times [O_3] \times [H_2O] \times f \qquad (3)$$

where f is the fraction of $O(^1D)$ that reacts with H_2O vapour to form OH, rather than being quenched to $O(^3P)$. Although
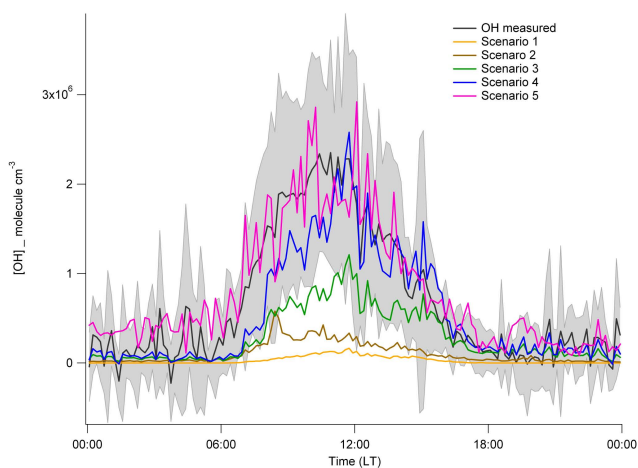
Fig. 2. A comparison of the measured mean diurnal [OH] profile ([OH]$_{meas.}$) (black line) with [OH]$_{calc.}$ calculated using the PSS approximation (Eq. 4) constrained to measured OH reactivity (k'_{OH}) for the loss term and with various OH source terms included – see text and Table 1 for further details on the different scenarios. The grey shading represents the 1σ standard deviation of the averaged OH profile, caused primarily by variability of the data from day-to-day due to changing atmospheric conditions, but also contains a contribution from instrumental precision.

$j(O^1D)$ and H_2O vapour concentrations were large, as expected in the tropics (peak $j(O^1D) \sim 3\times10^{-5}$ s^{-1} on average and [H_2O] ~ 2.5 % v/v), $p(OH)$ was limited by the low O_3 concentrations observed (peak [O_3] ~ 11 ppbv). If it is assumed that $p(OH)$ represents the *only* source of OH, i.e. $\Sigma_{OH_{sources}} = p(OH)$ (Scenario 1, Table 1), then the OH concentration, calculated by rearrangement of Eq. (2):

$$[OH]_{calc.} = \frac{\Sigma_{OH_{sources}}}{k'_{OH}} \quad (4)$$

would be expected to be very low given to the high value of k'_{OH}. Figure 2 shows a comparison of the average diurnal measured OH concentration ([OH]$_{meas}$) and [OH]$_{calc.}$; [OH]$_{calc}$ under-predicts [OH]$_{meas}$ by a factor of ~ 20 at noon. As k'_{OH} is measured (representing all OH sinks), the comparison shows that significant additional OH sources must be present in addition to production of OH from the reaction $O(^1D) + H_2O$ Eq. (3). Figure 2 also shows [OH]$_{calc}$ when all *known* OH sources are incorporated in Eq. (4), as detailed in Eq. (5). (C_5H_8 = isoprene) (Scenario 2, Table 1) (see Sect. 2 for further details on any estimates made on unmeasured species included in Eq. 5):

$$\Sigma_{OH_{sources}} = p(OH) + k_{NO+HO_2}[HO_2][NO] \quad (5)$$
$$+ k_{O_3+HO_2}[O_3][HO_2] + 0.26k_{O_3+C_5H_8}[O_3][C_5H_8]$$
$$+ 2j(H_2O_2)[H_2O_2] + j(CH_3OOH)[ROOH]$$

[OH]$_{calc}$ increases, predominantly due to inclusion of an OH source from HO_2+NO (78 % of the increase is due to inclusion of HO_2+NO) despite NO concentrations being very low; this OH source has the biggest impact on the PSS calculation during the early morning hours when NO peaks at ~ 200 pptv. Approximately 16 % of [OH]$_{calc}$ in Eq. (5) may be attributed to the photolysis of peroxides. Doubling the peroxide concentration increases the peak [OH]$_{calc}$ from 3.0×10^5 molecule cm^{-3} to 3.5×10^5 molecule cm^{-3}; halving the concentration reduces [OH]$_{calc}$ to 2.75×10^5 molecule cm^{-3}. Any uncertainties associated with the treatment of the photolysis of the peroxides, therefore, will only have a small impact on [OH]$_{calc}$ and do not alter the major findings from this work. Even with the inclusion of all *known* OH sources, [OH]$_{calc}$ still significantly under-predicts [OH]$_{meas}$ (by a factor of 10 at noon), demonstrating that there is still a large, uncharacterised OH source.

Recent theoretical calculations (Peeters et al., 2009; Da Silva et al., 2010) and laboratory studies (Paulot et al., 2009) have shown that OH may be regenerated during the OH initiated oxidation of isoprene under low NO$_x$ conditions, and if these are included as OH sources, (Scenario 3, Table 1) $\Sigma_{OH_{sources}}$ becomes:

$$\Sigma_{OH_{sources}} = p(OH) + k_{NO+HO_2}[HO_2][NO] \quad (6)$$
$$+ k_{O_3+HO_2}[O_3][HO_2] + 0.26k_{O_3+C_5H_8}[O_3][C_5H_8]$$
$$+ 2j(H_2O_2)[H_2O_2] + j(CH_3OOH)[ROOH]$$
$$+ \alpha k_{OH+C_5H_8}[OH][C_5H_8]$$

where α is the recycled yield of OH following the OH reaction with isoprene. [OH]$_{calc}$ increases considerably if $\alpha = 1$ as suggested by Peeters et al. (2009) is used (Scenario 3, Table 1) (Fig. 2), for which there is a direct OH source (0.03) and a larger OH source (0.97) from the rapid photolysis of photo-labile co-products and subsequent photochemistry. This mechanism also suggests an appreciable yield of HO_2 (0.7). Even with this new, considerable OH yield of 1 from OH initiated isoprene oxidation, OH concentrations are still under-predicted by ~ 63 % at midday. To achieve [OH]$_{calc}$/[OH]$_{meas} = 1$ during the afternoon and evening, approximately 2.7 OH radicals would need to be produced per isoprene molecule oxidised ($\alpha = 2.7$, Scenario 4, Table 1), potentially indicating that the OH yield from isoprene may actually be greater than 1. Stravrakou et al. (2010) propose that the rapid photolysis of the co-products formed during isoprene oxidation may actually yield 3 OH radicals. It should be noted, however, that OH concentrations are still under-predicted during the morning even with a yield of 2.7 from isoprene oxidation, as the isoprene concentrations are lower at this time, suggesting that the diurnal profile of the missing OH source(s) does not entirely follow the isoprene concentration profile. A similar finding has recently been reported by Lu et al. (2011) who found during analysis of HO$_x$ observations made during the PRIDE-PRD campaign that a dependence of the missing OH source upon isoprene could

not be strictly concluded. It is possible that similar mechanisms may also occur during the oxidative degradation of other biogenic species, for example mono-terpenes. A small subset of mono-terpenes were measured during the project; the concentrations of these species are insufficient to reconcile the missing OH source, however. High concentrations of unmeasured mono-terpenes would have had to be present in addition to those measured if these species are to account for the remaining missing OH source. P. M. Edwards (personal communication, 2011) found that model simulations of the OH reactivity measured during the campaign are able to reproduce the general trend in the observations, with the correlation between observed and calculated OH reactivity giving a linear correlation coefficient of $R = 0.9$; but the model under-predicts the magnitude of the observations by $\sim 53\%$. Although the direct reaction of OH with isoprene only accounts for $\sim 25\%$ of the total OH reactivity, the oxygenated VOCs generated from isoprene oxidation, account for a further 12% of the reactivity; this fraction increases further (to $\sim 27\%$) if the model is constrained to the OH observations and further still if the deposition lifetime of the oxygenated VOCs is increased from 1 to 3 days (to $\sim 55\%$). Under this third scenario the model is able to reproduce the magnitude of the reactivity observations to within 4%. These findings demonstrate the importance of the unconstrained oxidation products of the observed biogenic VOCs on OH reactivity and highlight that any uncertainties in the isoprene oxidation mechanism has the potential to impact modelled OH concentrations greatly; missing primarily emitted biogenics are not necessarily required to reconcile the observed OH reactivity.

The effect of including different OH sources on the calculated HO_2 concentration has been investigated using a full modelling approach (see Sect. 2.3), the results of which are shown in Fig. 3. Fuchs et al. (2011) have recently reported an interference in HO_2 measurements using a similar instrument as described in this paper. The interference, caused by the partial chemical conversion of certain RO_2 species to OH on addition of NO in the FAGE detection cell, has the potential to cause a systematic positive bias in HO_2 measurements and, therefore, HO_2 observations reported using the FAGE technique may be higher than the true ambient HO_2 concentrations. Under the operating conditions employed during the OP3 campaign, the University of Leeds FAGE instrument was relatively insensitive to detection of RO_2 species. During the campaign only one fluorescence cell was used to make alternate measurements of OH and HO_2 and conditions were optimised to maximise its sensitivity to OH. Under this configuration incomplete mixing of NO into the ambient airstream for the HO_2 titration was evident and resulted in low conversion of HO_2 to OH. Coupled with the high pumping capacity and, therefore, fast gas throughput of the fluorescence cell, this configuration effectively minimised the potential interference from ambient RO_2 species. Recent laboratory tests have revealed a 12% yield of HO_2 due to the decomposition of ethene-derived RO_2 in the presence of NO
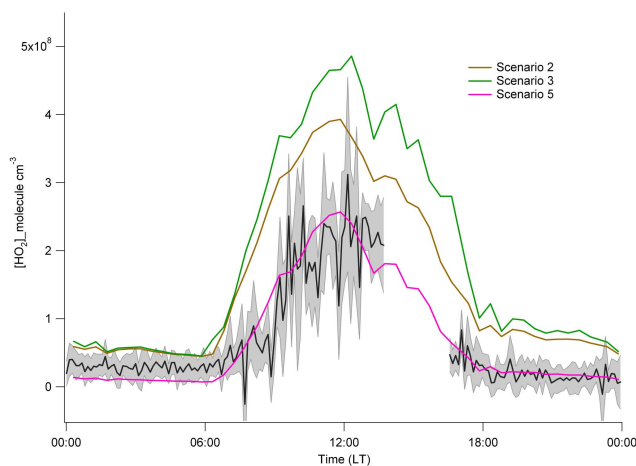

Fig. 3. A comparison of the measured diurnal HO_2 concentration profile from one day during OP3-III (black line) (grey shading highlights the 1σ variation in 10 s HO_2 signal that has been averaged to generate each 10 min data point) with modelled HO_2 from the MCM constrained to measurements made during OP3-I. The brown line represents the modelled HO_2 with OH sources defined by Scenario 2 (Table 1). The green line represents the modelled HO_2 with an additional OH and HO_2 source from including the Peeters mechanism (Scenario 3, Table 1). The pink line includes the standard OH source chemistry with an additional HO_2 to OH cycling step (equivalent to adding an additional 0.74 ppbv of NO) in the model (Scenario 5, Table 1).

in the FAGE detection cell under OP3 conditions. This provides an upper limit to the HO_2 yield from RO_2 species during OP3 as, under conditions optimised to maximise the interference signal, ethene-derived RO_2 species provided the largest HO_2 yield compared with other RO_2 species tested such as those derived from isoprene (yield of 10%), and higher alkanes (Whalley, 2011). Model simulations suggest that up to 2.1×10^8 molecule cm^{-3} of potentially interfering RO_2 species were present at solar noon during OP3 and thus up to 2.5×10^7 molecule cm^{-3} of the HO_2 concentration may be attributed to these species ($\sim 10\%$ of the total HO_2 signal). This small interference falls within the uncertainty of the HO_2 observations and should have very little impact on the following results:

A base run (brown line, Fig. 3) corresponding to all the OH sources that are included in Eq. (5), excluding any recycled OH from isoprene, overestimates the HO_2 observations taken during OP3-III (taking into account the small HO_2 interference would only serve to further increase this over-estimation). OH concentrations are significantly underpredicted by this model. Inclusion of the Peeters's mechanism (Peeters et al., 2009), which generates ~ 1 OH radical and ~ 0.7 HO_2 radicals per isoprene molecule oxidised leads to a considerable increase in the modelled HO_2 concentration ($\sim 20\%$ at noon) both as a consequence of an additional primary HO_2 source and an increase from VOC and

CO oxidation by OH. This mechanism causes the model to further over-predict the measured HO_2 concentration (green line, Fig. 3). This model still underestimates OH and, in line with the PSS calculation (and other modelling studies, e.g. Stavrakou et al., 2010), an OH yield from isoprene oxidation greater than unity is required to improve the modelled to measured agreement for OH. Such an increase in the OH yield from this mechanism only serves to increase HO_2, reducing the modelled to measured HO_2 agreement further. These results are consistent with the findings during the PRIDE-PRD (Hofzumahaus et al., 2009) and PROPHET-98 (Tan et al., 2001) campaigns and suggest that if OH and HO_2 are generated during the OH initiated oxidation of isoprene as postulated by Peeters et al. (2009) an additional mechanism that removes HO_2 must also occur to reconcile the measurements.

Hofzumahaus et al. (2009) found that additional recycling of RO_2 radicals to HO_2 and HO_2 to OH (via an unknown species X) could reconcile both OH and HO_2 concentrations during the PRIDE-PDR campaign, and this is incorporated in the rate of OH production via:

$$\Sigma_{OH_{sources}} = p(OH) + k_{NO+HO_2}[HO_2][NO] \qquad (7)$$
$$+ k_{O_3+HO_2}[O_3][HO_2] + 0.26 k_{O_3+C_5H_8}[O_3][C_5H_8]$$
$$+ 2j(H_2O_2)[H_2O_2] + j(CH_3OOH)[ROOH]$$
$$+ k_{X+HO_2}[X][HO_2]$$

To achieve $[OH]_{calc}/[OH]_{meas} = 1$ from an additional $HO_2 + X \rightarrow OH$ step under OP3 conditions, but without any OH recycling from isoprene, would require ~ 0.74 ppbv of unspecified reactant(s) (referred to as X) converting HO_2 to OH with the same rate coefficient by reaction with NO (or a HO_2 turnover rate to OH of ~ 6.5 s) (Scenario 5, Table 1 and Fig. 2). We have also included this additional recycling term in box model calculations of HO_2 as shown in Fig. 3 (pink line). Inclusion of the sources of OH given by Eq. (7) replicates the observed HO_2 concentrations well.

The additional recycling of OH may derive from a $HO_2 + RO_2$ reaction as suggested by Lelieveld et al. (2008). However, even if it is assumed that every RO_2 radical measured reacts with HO_2, a yield of ten OH radicals on average is required to replicate OH observations. Such a high OH radical yield from $RO_2 + HO_2$ reactions is not supported by the recent kinetic studies (Hasson et al., 2004; Dillon and Crowley, 2008). Only RO_2 radicals which contain a carbonyl functionality adjacent to the peroxy group have been found to regenerate significant OH upon reaction with HO_2 radicals, however, even the yield of OH from these reactions is only ~ 0.5 (Dillon and Crowley, 2008) demonstrating that other major OH recycling mechanisms must exist in addition to reconcile the OH concentrations observed.

It is possible that models may be missing both an OH source mechanism (for example OH regeneration during isoprene oxidation, Peeters et al., 2009) and a separate HO_2 loss mechanism. The fast HO_2 turnover rate of just a

~ 6.5 s suggests that the unknown HO_2 reactant must either be present at reasonable concentrations (e.g. with a reaction rate coefficient equal to $\sim 5 \times 10^{-12}$ cm^3 molecule^{-1} s^{-1} then ~ 1.3 ppbv of reactant would be required) or react extremely rapidly with HO_2 (e.g. if ~ 65 pptv of reactant was present then a reaction rate coefficient of $\sim 1 \times 10^{-10}$ cm^3 molecule^{-1} s^{-1} would be necessary). Although results from recent theoretical (Peeters et al., 2009; Da Silva et al., 2010; Nguyen et al., 2010) and laboratory studies (Dillon and Crowley, 2008) can help to suggest mechanisms that may help to reduce the modelled-measured discrepancy that is observed under high isoprene, low NO_x conditions, it seems clear that additional novel OH source mechanisms and HO_2 sink mechanisms are necessary to fully reconcile these recent radical measurements. Lu et al. (2011) draw similar conclusions from work analysing HO_x observations made in the Pearl river delta in China during the PRIDE-PRD campaign finding that the postulated isoprene mechanisms by Lelieveld et al. (2008) and Peeters and Mueller (2010) alone cannot explain the difference between measured and modelled OH at low NO_x; inclusion of the Peeters's mechanism was found to lead to an over-prediction of HO_2 by Lu and co-workers also.

4 Conclusions

Simultaneous field measurements of OH concentration, OH reactivity, and sources/sinks of OH in the Borneo rainforest at Bukit Atur directly show a large underestimate in OH sources in tropical forests. Under low NO_x conditions, an OH formation route is needed which can be reconciled with both observed OH and HO_2. This work indicates that an additional OH source from isoprene oxidation cannot resolve both the OH and HO_2 observations at this location unless an additional HO_2 sink mechanism is also included. An additional recycling mechanism that converts HO_2 to OH can account for the combined HO_x observations (without an additional OH source from isoprene oxidation). The impact of including the additional recycling step as a source of OH is an 88 % increase in [OH] at noon, significantly increasing the oxidising capacity of the tropical rainforest, and reducing the lifetime of CH_4 in these environments. This work demonstrates that moderate to high OH concentrations can be sustained in tropical rainforests, despite high biogenic emissions and low ozone, and highlights major uncertainties in the chemical mechanisms currently incorporated in models. Similar conclusions can be drawn from other work in this area. For example, global atmospheric chemistry models (ACMs) are not able to reconcile the observed isoprene concentrations with the measured isoprene emission rates; the emission rates incorporated tend to be lower than estimates based on direct emission measurements (Guenther, 2008). Higher emission rates in ACMs serve to dramatically deplete the OH radical concentration and lead to unrealistically

high concentrations of certain key atmospheric constituents (Poisson et al., 2000; Bey et al., 2001) pointing to major uncertainties in the isoprene oxidation mechanism. These uncertainties not only have major implication on the oxidising capacity, but lead to major uncertainties regarding oxidation products and their ultimate fates, e.g. secondary organic aerosol formation. The possibility of previously unidentified isoprene oxidation pathways, such as those discussed in this manuscript, will also undoubtedly impact any top-down estimates of isoprene emissions derived from satellite observations of isoprene oxidation products such as formaldehyde (Shim et al., 2005). This extremely useful approach to determining a global map of isoprene emissions relies heavily on an accurate understanding of isoprene oxidation.

To resolve these uncertainties, laboratory studies to test recently proposed theories are necessary, for example studies focussing on the regeneration of OH and HO_2 during isoprene oxidation or studies to determine HO_2 sinks. The ability to speciate individual RO_2 species and the measurement of more isoprene oxidation products in future field studies should provide further constraints for models and enable novel oxidation mechanisms to be validated.

Edited by: G. McFiggans

References

Archibald, A. T., Cooke, M. C., Utembe, S. R., Shallcross, D. E., Derwent, R. G., and Jenkin, M. E.: Impacts of mechanistic changes on HO_x formation and recycling in the oxidation of isoprene, Atmos. Chem. Phys., 10, 8097–8118, doi:10.5194/acp-10-8097-2010, 2010.

Bey, I., Jacob, D. J., Yantosca, R. M., Logan, J. A., Field, B. D., Fiore, A. M., Li, Q. B., Liu, H. G. Y., Mickley, L. J., and Schultz, M. G.: Global modeling of tropospheric chemistry with assimilated meteorology: Model description and evaluation, J. Geophys. Res.-Atmos., 106, 23073–23095, 2001.

Bloss, W. J., Evans, M. J., Lee, J. D., Sommariva, R., Heard, D. E., and Pilling, M. J.: The oxidative capacity of the troposphere: Coupling of field measurements of OH and a global chemistry transport model, Faraday Discuss., 130, 425–436, 2005.

Bohn, B., Corlett, G. K., Gillmann, M., Sanghavi, S., Stange, G., Tensing, E., Vrekoussis, M., Bloss, W. J., Clapp, L. J., Kortner,

M., Dorn, H. P., Monks, P. S., Platt, U., Plass-Dulmer, C., Mihalopoulos, N., Heard, D. E., Clemitshaw, K. C., Meixner, F. X., Prevot, A. S. H., and Schmitt, R.: Photolysis frequency measurement techniques: results of a comparison within the ACCENT project, Atmos. Chem. Phys., 8, 5373–5391, doi:10.5194/acp-8-5373-2008, 2008.

Butler, T. M., Taraborrelli, D., Fischer, C. B. H., Harder, H., Martinez, M., Williams, J., Lawrence, M. G., and Lelieveld, J.: Improved simulation of isoprene oxidation chemistry with the ECHAM5/MESSy chemistry-climate model: lessons from the GABRIEL airborne field campaign, Atmos. Chem. Phys., 8, 4529–4546, doi:10.5194/acp-8-4529-2008, 2008.

Carslaw, N., Creasey, D. J., Harrison, D., Heard, D. E., Hunter, M. C., Jacobs, P. J., Jenkin, M. E., Lee, J. D., Lewis, A. C., Pilling, M. J., Saunders, S. M., and Seakins, P. W.: OH and HO_2 radical chemistry in a forested region of north-western Greece, Atmos. Environ., 35, 4725–4737, 2001.

Da Silva, G., Graham, C., and Wang, Z.-F.: Unimolecular beta-hydroxyperoxy radical decompostion with OH recycling in the photochemical oxidation of isoprene, Environ. Sci. Tech., 44, 250–256, 2010.

Dillon, T. J. and Crowley, J. N.: Direct detection of OH formation in the reactions of HO_2 with $CH_3C(O)O_2$ and other substituted peroxy radicals, Atmos. Chem. Phys., 8, 4877–4889, doi:10.5194/acp-8-4877-2008, 2008.

Ehhalt, D. H. and Rohrer, F.: The tropospheric cycle of H_2: a critical review, Tellus B – Chem. Phys. Meteorol., 61, 500–535, 2009.

Fleming, Z. L., Monks, P. S., Rickard, A. R., Heard, D. E., Bloss, W. J., Seakins, P. W., Still, T. J., Sommariva, R., Pilling, M. J., Morgan, R., Green, T. J., Brough, N., Mills, G. P., Penkett, S. A., Lewis, A. C., Lee, J. D., Saiz-Lopez, A., and Plane, J. M. C.: Peroxy radical chemistry and the control of ozone photochemistry at Mace Head, Ireland during the summer of 2002, Atmos. Chem. Phys., 6, 2193–2214, doi:10.5194/acp-6-2193-2006, 2006.

Fuchs, H., Bohn, B., Hofzumahaus, A., Holland, F., Lu, K., Nehr, S., Rohrer, F., and Wahner, A.: Detection of HO_2 by laser-induced fluorescence: Calibration and interferences from RO_2 radicals, Atmos. Meas. Tech., 4, 1209–1225, doi:10.5194/amt-4-1209-2011, 2011.

Govaerts, Y. M., Lattanzio, A., Taberner, M., and Pinty, B.: Generating global surface albedo products from multiple geostationary satellites, Remote Sens. Environ., 112, 2804–2816, 2008.

Guenther, A.: Atmospheric chemistry: Are plant emissions green?, Nature, 452, 701–702, 2008.

Hairer, E. and Wanner, G.: Solving Ordinary Differential Equations: Stiff and Differential-Algerbraic Problems, Berlin, Germany, 1991.

Hasson, A. S., Tyndall, G. S., and Orlando, J. J.: A product yield study of the reaction of HO_2 radicals with ethyl peroxy ($C_2H_5O_2$), acetyl peroxy ($CH_3C(O)O_2$), and acetonyl peroxy ($CH_3C(O)CH_2O_2$) radicals, J. Phys. Chem. A, 108, 5979–5989, 2004.

Heard, D. E. and Pilling, M. J.: Measurement of OH and HO_2 in the troposphere, Chem. Rev., 103, 5163–5198, 2003.

Hewitt, C. N., Lee, J. D., MacKenzie, A. R., Barkley, M. P., Carslaw, N., Carver, G. D., Chappell, N. A., Coe, H., Collier, C., Commane, R., Davies, F., Davison, B., Di Carlo, P., Di Marco, C. F., Dorsey, J. R., Edwards, P. M., Evans, M. J.,

Fowler, D., Furneaux, K. L., Gallagher, M., Guenther, A., Heard, D. E., Helfter, C., Hopkins, J., Ingham, T., Irwin, M., Jones, C., Karunaharan, A., Langford, B., Lewis, A. C., Lim, S. F., MacDonald, S. M., Mahajan, A. S., Malpass, S., McFiggans, G., Mills, G., Misztal, P., Moller, S., Monks, P. S., Nemitz, E., Nicolas-Perea, V., Oetjen, H., Oram, D. E., Palmer, P. I., Phillips, G. J., Pike, R., Plane, J. M. C., Pugh, T., Pyle, J. A., Reeves, C. E., Robinson, N. H., Stewart, D., Stone, D., Whalley, L. K., and Yin, X.: Overview: oxidant and particle photochemical processes above a south-east Asian tropical rainforest (the OP3 project): introduction, rationale, location characteristics and tools, Atmos. Chem. Phys., 10, 169-199, doi:10.5194/acp-10-169-2010, 2010.

Hofzumahaus, A., Rohrer, F., Lu, K., Bohn, B., Brauers, T., Chang, C., Fuchs, H., Holland, F., Kita, K., Kondo, Y., Li, X., Lou, S., Shao, M., Zeng, L., Wahner, A., and Zhang, Y.: Amplified trace gas removal in the troposphere, Science, 324, 1702–1704, 2009.

Hopkins, J. R., Lewis, A. C., and Read, K. A.: A two-column method for long-term monitoring of non-methane hydrocarbons (NMHCs) and oxygenated volatile organic compounds (o-VOCs) J. Environ. Mon., 5, 8–13, 2003.

Ingham, T., Goddard, A., Whalley, L. K., Furneaux, K. L., Edwards, P. M., Seal, C. P., Self, D. E., Johnson, G. P., Read, K. A., Lee, J. D., and Heard, D. E.: A flow-tube based laser-induced fluorescence instrument to measure OH reactivity in the troposphere, Atmos. Meas. Tech., 2, 465–477, doi:10.5194/amt-2-465-2009, 2009.

Kubistin, D., Harder, H., Martinez, M., Rudolf, M., Sander, R., Bozem, H., Eerdekens, G., Fischer, H., Gurk, C., Klupfel, T., Konigstedt, R., Parchatka, U., Schiller, C. L., Stickler, A., Taraborrelli, D., Williams, J., and Lelieveld, J.: Hydroxyl radicals in the tropical troposphere over the Suriname rainforest: comparison of measurements with the box model MECCA, Atmos. Chem. Phys., 10, 9705–9728, doi:10.5194/acp-10-9705-2010, 2010.

Lelieveld, J., Peters, W., Dentener, F. J., and Krol, M. C.: Stability of tropospheric hydroxyl chemistry, J. Geophys. Res. Atmos., 107(D16), 4715, doi:10.1029/2001JD001289, 2002.

Lelieveld, J., Dentener, F. J., Peters, W., and Krol, M. C.: On the role of hydroxyl radicals in the self-cleansing capacity of the troposphere, Atmos. Chem. Phys., 4, 2337–2344, doi:10.5194/acp-4-2337-2004, 2004.

Lelieveld, J., Butler, T. M., Crowley, J. N., Dillon, T. J., Fischer, H., Ganzeveld, L., Harder, H., Lawrence, M. G., Martinez, M., Taraborrelli, D., and Williams, J.: Atmospheric oxidation capacity sustained by a tropical forest, Nature, 452, 737–740, 2008.

Lu, K. D., Rohrer, F., Holland, F., Fuchs, H., Bohn, B., Brauers, T., Chang, C. C., Häseler, R., Hu, M., Kita, K., Kondo, Y., Li, X., Lou, S. R., Nehr, S., Shao, M., Zeng, L. M., Wahner, A., Zhang, Y. H., and Hofzumahaus, A.: Observation and modelling of OH and HO$_2$ concentrations in the Pearl River Delta 2006: a missing OH source in a VOC rich atmosphere, Atmos. Chem. Phys. Discuss., 11, 11311–11378, doi:10.5194/acpd-11-11311-2011, 2011.

Madronich, S. and Flocke, S.: Handbook of Environmental Chemistry, edited by: Boule, P., Springer, New York, USA, 1–26, 1998.

Malkin, T. L., Goddard, A., Heard, D. E., and Seakins, P. W.: Measurements of OH and HO$_2$ yields from the gas phase

ozonolysis of isoprene, Atmos. Chem. Phys., 10, 1441–1459, doi:10.5194/acp-10-1441-2010, 2010.

Martin, M. V., Honrath, R. E., Owen, R. C., Pfister, G., Fialho, P., and Barata, F.: Significant enhancements of nitrogen oxides, black carbon, and ozone in the North Atlantic lower free troposphere resulting from North American boreal wildfires, J. Geophys. Res. Atmos., 111, D23S60, doi:10.1029/2006JD007530, 2006.

Martinez, M., Harder, H., Kubistin, D., Rudolf, M., Bozem, H., Eerdekens, G., Fischer, H., Gurk, C., Klupfel, T., Konigstedt, R., Parchatka, U., Schiller, C. L., Stickler, A., Williams, J., and Lelieveld, J.: Hydroxyl radicals in the tropical troposphere over the Suriname rainforest: airborne measurements, Atmos. Chem. Phys., 10, 3759–3773, doi:10.5194/acp-10-3759-2010, 2010.

Monks, P. S.: Gas-phase radical chemistry in the troposphere, Chem. Soc. Rev., 34, 376–395, 2005.

Nguyen, T. L., Vereecken, L., and Peeters, J.: HO$_x$ Regeneration in the Oxidation of Isoprene III: Theoretical Study of the key Isomerisation of the Z-delta-hydroxy-peroxy Isoprene Radicals, Chem. Phys. Chem., 11, 3996–4001, 2010.

Novelli, P. C., Lang, P. M., Masarie, K. A., Hurst, D. F., Myers, R., and Elkins, J. W.: Molecular hydrogen in the troposphere: Global distribution and budget, J. Geophys. Res. Atmos., 104, 30427–30444, 1999.

Paulot, F., Crounse, J. D., Kjaergaard, H. G., Kurten, A., St Clair, J. M., Seinfeld, J. H., and Wennberg, P. O.: Unexpected Epoxide Formation in the Gas-Phase Photooxidation of Isoprene, Science, 325, 730–733, 2009.

Peeters, J., Nguyen, T. L., and Vereecken, L.: HO$_x$ radical regeneration in the oxidation of isoprene, Phys. Chem. Chem. Phys., 28, 5935–5939, 2009.

Pike, R. C., Lee, J. D., Young, P. J., Carver, G. D., Yang, X., Warwick, N., Moller, S., Misztal, P., Langford, B., Stewart, D., Reeves, C. E., Hewitt, C. N., and Pyle, J. A.: NO$_x$ and O$_3^-$ above a tropical rainforest: an analysis with a global and box model, Atmos. Chem. Phys., 10, 10607–10620, doi:10.5194/acp-10-10607-2010, 2010.

Poisson, N., Kanakidou, M., and Crutzen, P. J.: Impact of non-methane hydrocarbons on tropospheric chemistry and the oxidizing power of the global troposphere: 3-dimensional modelling results, J. Atmos. Chem., 36, 157–230, 2000.

Pugh, T. A. M., MacKenzie, A. R., Hewitt, C. N., Langford, B., Edwards, P. M., Furneaux, K. L., Heard, D. E., Hopkins, J. R., Jones, C. E., Karunaharan, A., Lee, J., Mills, G., Misztal, P., Moller, S., Monks, P. S., and Whalley, L. K.: Simulating atmospheric composition over a South-East Asian tropical rainforest: performance of a chemistry box model, Atmos. Chem. Phys., 10, 279–298, doi:10.5194/acp-10-279-2010, 2010.

Pugh, T. A. M., MacKenzie, A. R., Langford, B., Nemitz, E., Misztal, P. K., and Hewitt, C. N.: The influence of small-scale variations in isoprene concentrations on atmospheric chemistry over a tropical rainforest, Atmos. Chem. Phys., 11, 4121–4134, doi:10.5194/acp-11-4121-2011, 2011.

Ren, X. R., Olson, J. R., Crawford, J. H., Brune, W. H., Mao, J. Q., Long, R. B., Chen, Z., Chen, G., Avery, M. A., Sachse, G. W., Barrick, J. D., Diskin, G. S., Huey, L. G., Fried, A., Cohen, R. C., Heikes, B., Wennberg, P. O., Singh, H. B., Blake, D. R., and Shetter, R. E.: HO$_x$ chemistry during INTEX-A 2004: Observation, model calculation, and com-

parison with previous studies, J. Geophys. Res. Atmos., 113, D05310, doi:10.1029/2007JD009166, 2008.

Salisbury, G., Rickard, A. R., Monks, P. S., Allan, B. J., Bauguitte, S., Penkett, S. A., Carslaw, N., Lewis, A. C., Creasey, D. J., Heard, D. E., Jacobs, P. J., and Lee, J. D.: Production of peroxy radicals at night via reactions of ozone and the nitrate radical in the marine boundary layer, J. Geophys. Res. Atmos., 106, 12669–12687, 2001.

Shim, C., Wang, Y. H., Choi, Y., Palmer, P. I., Abbot, D. S., and Chance, K.: Constraining global isoprene emissions with Global Ozone Monitoring Experiment (GOME) formaldehyde column measurements, J. Geophys. Res.-Atmos., 110, D24301, doi:10.1029/2004JD005629, 2005.

Sinha, V., Williams, J., Crowley, J. N., and Lelieveld, J.: The comparative reactivity method - a new tool to measure total OH reactivity in ambient air, Atmos. Chem. Phys., 8, 2213–2227, doi:10.5194/acp-8-2213-2008, 2008.

Stavrakou, T., Peeters, J., and Muller, J. F.: Improved global modelling of HO_x recycling in isoprene oxidation: evaluation against the GABRIEL and INTEX-A aircraft campaign measurements, Atmos. Chem. Phys., 10, 9863–9878, doi:10.5194/acp-10-9863-2010, 2010.

Stone, D., Evans, M. J., Commane, R., Ingham, T., Floquet, C. F. A., McQuaid, J. B., Brookes, D. M., Monks, P. S., Purvis, R., Hamilton, J. F., Hopkins, J., Lee, J., Lewis, A. C., Stewart, D., Murphy, J. G., Mills, G., Oram, D., Reeves, C. E., and Heard, D. E.: HO_x observations over West Africa during AMMA: impact of isoprene and NO_x, Atmos. Chem. Phys., 10, 9415–9429, doi:10.5194/acp-10-9415-2010, 2010.

Tan, D., Faloona, I., Simpas, J. B., Brune, W., Shepson, P. B., Couch, T. L., Sumner, A. L., Carroll, M. A., Thornberry, T., Apel, E., Riemer, D., and Stockwell, W.: HO_x budgets in a deciduous forest: Results from the PROPHET summer 1998 campaign, J. Geophys. Res. Atmos., 106, 24407–24427, 2001.

Thornton, J. A., Wooldridge, P. J., Cohen, R. C., Martinez, M., Harder, H., Brune, W. H., Williams, E. J., Roberts, J. M., Fehsenfeld, F. C., Hall, S. R., Shetter, R. E., Wert, B. P., and Fried, A.: Ozone production rates as a function of NO_x abundances and HO_x production rates in the Nashville urban plume, J. Geophys. Res. Atmos., 107(D12), doi:10.1029/2001JD000932, 2002.

Whalley, L. K., Furneaux, K. L., Goddard, A., Lee, J. D., Mahajan, A., Oetjen, H., Read, K. A., Kaaden, N., Carpenter, L. J., Lewis, A. C., Plane, J. M. C., Saltzman, E. S., Wiedensohler, A., and Heard, D. E.: The chemistry of OH and HO_2 radicals in the boundary layer over the tropical Atlantic Ocean, Atmos. Chem. Phys., 10, 1555–1576, doi:10.5194/acp-10-1555-2010, 2010.

Whalley, L. K.: The sensitivity of FAGE instruments to RO_2 radicals, interactive comment C350–C351 on Fuchs, H., Bohn, B., Hofzumahaus, A., Holland, F., Lu, K. D., Nehr, S., Rohrer, F., and Wahner A.: Detection of HO_2 by laser-induced fluorescence: calibration and interferences from RO_2 radicals, Atmos. Meas. Tech., 4, 1209–1225, doi:10.5194/amt-4-1209-2011, 2011.

Wild, O., Law, K. S., McKenna, D. S., Bandy, B. J., Penkett, S. A., and Pyle, J. A.: Photochemical trajectory modeling studies of the North Atlantic region during August 1993, J. Geophys. Res.-Atmos., 101, 29269–29288, 1996.